Special Issue
"Progress of Theoretical and Computational Biophysics"

Vol. 16, pp. 280–286 (2019)
doi: 10.2142/biophysico.16.0_280

Biophysics and Physicobiology

https://www.jstage.jst.go.jp/browse/biophysico/

Regular Article

All Atom Motion Tree detects side chain-related motions and their coupling with domain motion in proteins

Ryotaro Koike and Motonori Ota

Graduate School of Informatics, Nagoya University, Nagoya, Aichi 464-8601, Japan

Received July 1, 2019; accepted July 25, 2019

Structural changes of proteins are closely related with their molecular function. We previously developed a computational tool, Motion Tree (MT), to compare protein structures and describe structural changes using solely the Cα atoms. Here, we have extended MT to incorporate all heavy atoms to analyze side chain-related (SCR) motions. All Atom Motion Tree (AAMT) was applied to 76 proteins that exhibited a simple domain motion identified by MT. AAMT also detected 921 SCR motions. We examined the coupling of domain and SCR motions and classified the structural changes in terms of coupling. The statistical results indicated that it is common for coupled SCR motions to also couple with the domain motion. The classification correlates properties of domain motions and SCR motions. The AAMT results suggest that a large domain motion with a sizable domain boundary is accompanied by SCR motions composed of more than a single residue, which induces further couplings of SCR motions.

Key words: Rigid-body motion, structural change, conformational change

Corresponding author: Ryotaro Koike, Graduate School of Informatics, Nagoya University, Furo-cho, Chikusa-ku, Nagoya, Aichi 464-8601, Japan.
e-mail: rkoike@i.nagoya-u.ac.jp

Structural changes of proteins are closely related with their molecular function [1–4]. Currently, a number of computational methods to investigate protein structural changes by taking protein structures from the PDB [5,6] have been proposed [7–16]. We previously developed Motion Tree (MT), which compares two structures of an identical protein using distance matrices of Cα atoms [17] and detects rigid bodies in structures [11]. Rigid bodies are the units of structural change and act as the building blocks in the movement. A remarkable feature of MT is its ability to detect various rigid bodies, ranging from a small rigid body for loop motion to large rigid bodies such as domain motion. In previous work, MT revealed that a number of proteins including kinases and ATP synthase exhibit both local and domain motions [11]. The exhaustive identification of rigid bodies clearly aids our understanding of the mechanism of their molecular function in terms of structural changes. However, subtle movements, e.g., side chain motions, are also known to play important roles in protein function [18]. This fact strongly motivated us to extend MT to incorporate side chain atoms.

In this study, we developed a new Motion Tree that uses all heavy atoms of protein structures. The All Atom Motion Tree (AAMT) detects a wide range of rigid bodies, and we identify a number of rigid bodies composed of side chain atoms. Figure 1 illustrates the two Motion Trees, MT and

◀ **Significance** ▶

To detect small and large structural changes in proteins we have developed All Atom Motion Tree (AAMT), which compares distinct structures of a protein using all heavy atoms including side chains. AAMT identified a number of side chain-related (SCR) motions in addition to domain motions. We analyzed coupling of domain and SCR motions in many proteins. The statistics indicate that couplings among SCR motions are common, as are those of SCR and domain motions. Our results demonstrate that AAMT is a useful tool to evaluate the coupling of local and global motions and their consistency with protein function.

©2019 THE BIOPHYSICAL SOCIETY OF JAPAN

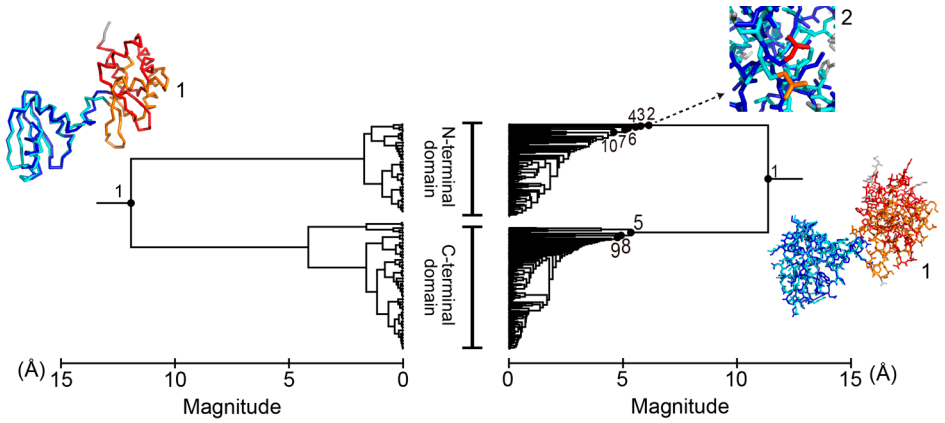

Figure 1 The All Atom Motion Tree (AAMT) and original Motion Tree (MT) of the arginine repressor. The two distinct structures (chains D and F in PDB entry 1f9n) were compared. In MT (left), there is one effective node (black circle with node number "1"), which presents a domain motion between N- and C-terminal domains. The domain motion is shown by the superposition of the Cα structures with the node number 1. The movement of a smaller rigid body (red (F chain) and orange portions (D)) is highlighted by superimposing the larger rigid body (blue (F) and cyan (D)). In contrast, there are ten effective nodes in AAMT (right). The domain motion at node 1 is illustrated by the structures in an all-atom-stick model. Among the other motions at nodes 2–10, the motion at node 2 is shown.

AAMT, for the arginine repressor [19]. In each tree, a root is the whole protein and leafs are residues (MT) or atoms (AAMT). Rigid bodies are hierarchically shown in the dendrogram, and each node shows larger and smaller rigid bodies that have divided from an ancestral rigid body, representing their relative movement. Clearly, MT detects only a domain motion at node 1, whereas AAMT detects additional motions (nodes 2–10). We applied AAMT to proteins that exhibit a simple domain motion (e.g., Fig. 1). The side chain-related (SCR) motions are defined as rigid bodies in AAMT, such as the motion at node 2 in Figure 1. In particular, we focused on the coupling of a domain motion with SCR motions and that among SCR motions.

Materials and Methods

All Atom Motion Tree

The AAMT is a simple extension of the original MT. Here, AAMT uses all heavy atoms in protein structures, whereas MT uses only Cα atoms. To represent a protein structure, we employed a distance matrix, in which the distances of any pair of "heavy atoms" are calculated as matrix elements. The difference matrix of two distance matrices describes a structural change between two different structures of an identical protein. Taking the elements of the distance-difference matrix as a dissimilarity matrix, we performed hierarchical clustering to obtain a dendrogram named the "All Atom Motion Tree".

Initially, in hierarchical clustering each atom of the protein comprises a cluster. Based on the dissimilarity matrix, the most similar pair of clusters is merged and the dissimilarity matrix is updated. These steps are repeated until all the atoms are clustered. We introduced two special treatments in this clustering process. One treatment is the definition of dissimilarity. Consider two clusters C_1 and C_2. In complete-linkage clustering, the maximum distance-difference value in two clusters is used as the dissimilarity measure. However, we noticed previously that the single maximal value often overemphasized the dissimilarity [11]. In AAMT, we gathered the largest 4% of all the distance-difference values in C_1 vs. C_2 and regarded their average as the dissimilarity between C_1 and C_2 (see Supplementary materials). Another treatment is a criterion for merging two clusters. We confirm the spatial proximity of two clusters to ensure that the new cluster can be connected in space. The merge is accepted when the closest pair of atoms from each of the clusters is within 4.0 Å (essentially the van der Waals radii of two atoms plus 1.0 Å). Otherwise, the next similar clusters are examined. To ensure the ancestral node has a higher dissimilarity measure than the descendant nodes (to avoid the inversion of nodes), we added a restriction to the dissimilarity measure (see Supplementary materials).

When analyzing AAMT, we introduced effective nodes as a label of significant rigid-body motions. At an effective node, a rigid body consisting of more than 10 atoms is divided into two rigid bodies, each containing three or more atoms. The magnitude of the effective node is more than 4.5 Å. The threshold of the magnitude is determined so that AAMT can detect almost the same domain motions identified by MT (see Supplementary materials). Only rigid bodies at the effective nodes were investigated in this study.

Dataset

In previous work, 104 proteins exhibiting a simple domain motion were identified by MT, in which only an effective node that divides all residues into two domains (each composed of at least 30 residues) existed. Among them, we filtered some irregular structures and selected 87 proteins. The

irregular structures are old PDB structures that are obsolete from the PDB, structures mostly composed of only Cα atoms and structures containing isolated atoms that prevent clusters meeting the spatial-proximity condition. The set of 87 proteins were used to determine the adjustable parameters (see Supplementary materials).

An aim of this study was to estimate the coupling of the known domain motions that were identified by MT and other side chain-related motions (SCR motion; see next section) that were identified firstly by AAMT. In the analyzing process (see next section), we realized that some proteins were not suitable for this aim, where the domain motion detected by AAMT was apparently different from that of MT, or AAMT identified additional domain motions. Finally, 76 structural pairs of proteins comprise the dataset in this study. The list of all pairs is shown in Supplementary Table S1.

Domain and side chain-related (SCR) motions

We examined rigid-body motions detected by AAMT. Basically, we assumed the aforementioned 87 samples exhibit one domain motion, and anticipated them to show more additional motions, in which side chains were substantially included in rigid bodies. We define the domain motion of AAMT when it corresponds to the known domain motion detected by MT. The residues (Cα atoms) in the rigid bodies of AAMT were compared with those of MT. We considered that both motions were essentially the same if the overlap of residues was more than 75%. Among the remaining motions, we visually examined smaller rigid bodies at the nodes if the sizes were 10 or more residues, and discriminated four motions as additional "domain motions" that were not detected by MT. All the remaining motions were defined as SCR motions. Samples showing additional domain motions were removed. Thus, all samples in the dataset exhibited only one domain motion and SCR motions if existed.

Results and Discussion

Statistics: coupling of motions

We illustrated AAMTs for 76 structural pairs of proteins. An effective node corresponding to the domain motion was identified in each of the trees. In addition, 921 effective nodes corresponding to SCR motions were detected in 73 trees. No SCR motions were observed in only three proteins. The 921 nodes are basically rigid-body motions ascribed to side chain atoms. Node 2 of the right tree in Figure 1 is an example. The average size of smaller rigid bodies is 9.0 atoms of 1.7 residues. The average occupancy of side chain atoms in the rigid bodies is 86.8%.

We simply examined the contact of rigid bodies (nearest atom distance <4.0 Å in either of two structures or both) to evaluate the coupling of domain and SCR motions. SCR and domain motions were coupled when the smaller rigid body of a SCR motion had contacts with both rigid bodies of the domain motion (i.e., around the rigid-body boundary of the domain motion). Two SCR motions are coupled when smaller rigid bodies of distinct SCR motions form a contact. The rigid bodies in contact are expected to have great influence on their dynamics each other through the direct interaction. Therefore, we assume motions are coupled when the rigid bodies are in contact. All 76 protein structural changes were categorized in terms of coupling of domain and SCR motions, according to the degree of the coupling, as follows: (1) no SCR motion coupled with the domain motion (abbreviation: no-SCR); (2) only a single SCR motion coupled with the domain motion, but it has no other coupled-SCR motions (single-SCR); (3) multiple SCR motions coupled with the domain motion, but they are uncoupled (multi-SCR-uncoupled); and (4) others: multiple SCR motions are coupled with each other, and at least one of them couples with the domain motion (multi-SCR-coupled). In this category, the cluster of coupled SCR motions may include SCR motions that are not directly coupled with domain motions. These four groups are schematically shown in Figure 2a, and the statistics are summarized in Figure 2b. The multi-SCR-coupled category is the largest with almost half of the proteins belonging this category (35 proteins). We concluded that the coupling of domain motion and a number of SCR motions is common.

Properties of domain motions accompanying SCR motions

We hypothesized that the four types of SCR motions are characterized by some properties of domain motions and explored these characteristic features. The magnitude of the domain motion (the horizontal axis of AAMT at the effective node) indicates the degree of the motion and was found to be approximately proportional to the root-mean-square-deviation (RMSD) of structural changes. We found that this magnitude was an indicator to describe the degree of coupling (Fig. 3a). The largest average magnitude of domain motion is observed in the multi-SCR-coupled category (red box). The average magnitudes gradually decrease from groups 3 to 2 (yellow and green boxes), and the smallest value is observed for the no-SCR category (black box). This indicates that a large domain motion has a strong affect on its rigid-body boundary, which results in many coupled SCR motions. Additionally, the size of the rigid-body boundary of the domain motion affects the coupling of domain and SCR motions (Fig. 3b). The size was estimated by the number of contacting residues between rigid bodies of domain motions. In the multi-SCR-uncoupled and coupled groups (yellow and red boxes), the rigid-body boundaries are larger than those observed for the no-SCR and single-SCR groups (black and green boxes). This result indicates that the domain motion with large rigid-body boundaries induces more SCR motions around boundaries.

Remarkably, domain motion with a large structural change and a sizable rigid-body boundary is accompanied by a number of SCR motions. Next, the properties that distinguish the multi-SCR-coupled and uncoupled groups were explored.

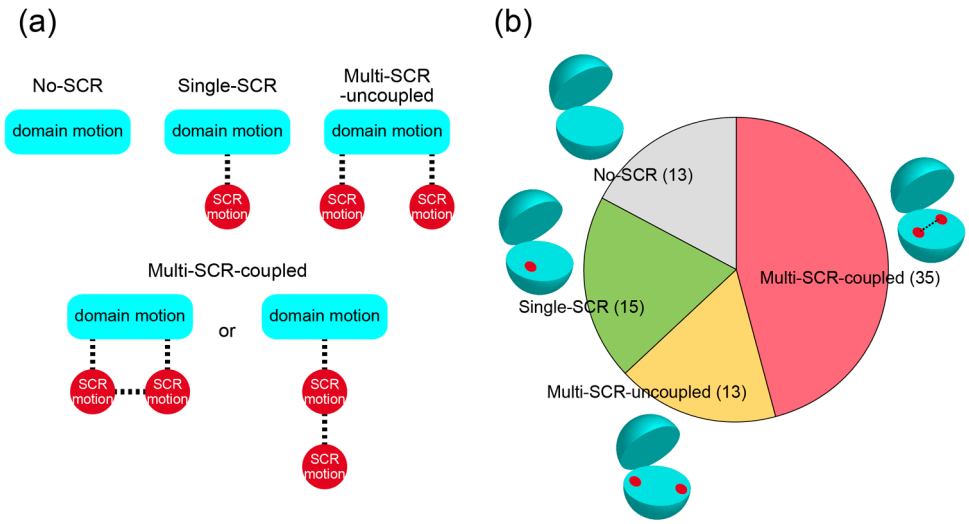

Figure 2 Classification of structural changes based on the coupling of domain and side chain-related (SCR) motions. (a) The four categories of structural change are represented using schematic diagrams. The cyan box and red circle present domain and SCR motions, respectively. The dotted line indicates the coupling between them. (b) Statistics of the four motions. The number of proteins is shown in parentheses.

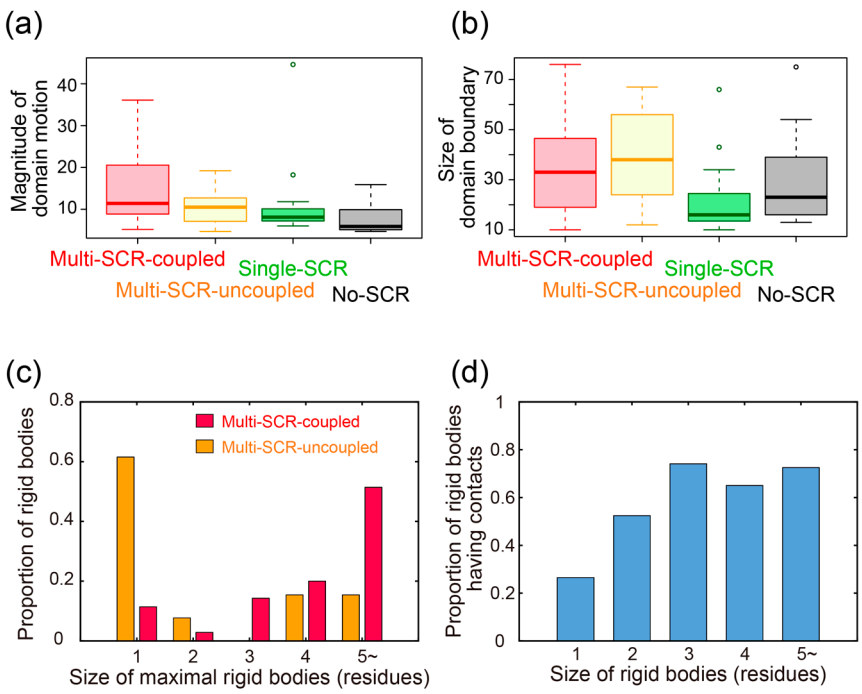

Figure 3 Properties of domain and SCR motions. (a) Box plot of the magnitude of the domain motion in the four categories. (b) Box plot of the rigid-body boundary size of the domain motion. (c) Distributions of the maximal rigid-body size (number of residues) of SCR motion in the multi-SCR-coupled (red) and -uncoupled (orange) groups. We measured how many residues constituted a rigid body of SCR motion that was coupled with domain motion. The maximal size was selected when many SCR motions were coupled with a domain motion in a sample. (d) Coupling (contact) rate of the rigid body of SCR motions with those of other SCR motions against the rigid-body size (residues). In principle, a sizable rigid body of a SCR motion can be divided, and another SCR motion is detected. However, such a division was rare in the dataset (only 33 SCR motions in 921).

The difference between the groups depends on whether the rigid body of the SCR motion, at the rigid-body boundary of the domain motion and coupled with the domain motion, contacts with other SCR motions, and then we analyzed them. The sizes of the smaller rigid bodies of SCR motions were calculated and we took the maximal value among those of multiple SCR motions as the representative of protein structural change. The number of residues in the rigid body represents its size. If an atom or part of a residue constitutes a rigid body, the residue is regarded to be in the rigid body. The maximal rigid-body sizes were found to differ between the multi-SCR-coupled and uncoupled groups, and the size distributions are shown in Figure 3c. Rigid bodies composed of five or more residues are frequently observed in the multi-SCR-coupled, whereas the majority of the maximum rigid bodies in the multi-SCR-uncoupled group are only composed of atoms within a residue. This result suggests that SCR motions of large rigid bodies at the rigid-body boundary of the domain motion are linked with other SCR motions. To confirm this observation, we gathered smaller rigid bodies of all SCR motions regardless of their locations at the rigid-body boundary of domain motion and investigated their contact (coupling). The result is shown in Figure 3d. The plot clearly shows that small rigid bodies composed of a residue tend to be isolated from other rigid bodies; only 27% of them form a contact with other rigid bodies. In contrast, rigid bodies that consist of two or more residues generally form contacts with other rigid bodies, with more than half of the rigid bodies composed of only two residues having contacts with other rigid bodies.

In summary, when a large domain motion occurs it is accompanied by some structural modifications around the domain boundary. The modification includes the SCR motion composed of two or more residues at the boundary, which is also accompanied by additional SCR motions. Consequently, the coupling of multiple SCR motions is induced at a sizable domain boundary.

An example: couplings of domain and SCR motions

AAMT illustrating the structural change between two conformers 1 (A chain in PDB entry 1jzo [20]) and 2 (A chain in 1tjd [21]) of the disulfide bond isomerase DsbC is shown in Figure 4a. The effective node 1 represents the domain motion between the N-terminal and C-terminal domains. The inter-domain flexibility is considered to play an important role in the recognition of substrate proteins [21]. The other 10 effective nodes represent SCR motions. Nodes 3 and 4 are the SCR motions coupled with the domain motion. The SCR motion at node 3 forms a large cluster of coupled SCR motions with nodes 2, 5, 8 and 9, and their relationship is illustrated in Figure 4b (see following paragraphs for details). The other nodes, 6, 7, 10 and 11, respectively show the SCR motions of V158, H102, D1 and K28, which are located distal from the rigid-body boundary of the domain motion and are also isolated from each other.

The cluster of coupled SCR motions (nodes 2, 3, 5, 8 and 9) is localized near the rigid-body boundary of the domain motion. Node 3 is a side chain motion of N33. In Figure 4c, two rigid bodies of N33 from conformers 1 and 2 are shown in dark green and green, respectively. The Cβ atom of A172 and Cδ1 of L128 (white spheres) belong to the C-terminal domain. In conformer 2, the two atoms contact with the end of the N33 side chain (green). In contrast, in conformer 1, N33 (dark green) rotates toward and into the N-terminal domain, and this change in conformation correlates with the shift of the side chain of K15 at node 8 (red and orange for conformers 1 and 2). The K15 side chain (red) is in close proximity to the reoriented N33 (dark green) and these two residues are almost parallel in conformer 1, whereas in conformation 2 there are no contacts. The conformational shift of K15 arises from a rotation in the dihedral angle ψ from 111° in conformer 1 to −88° in conformer 2. This may influence the SCR motion of S16 and S17 (blue and cyan for conformers 1 and 2, respectively, in Fig. 4d) at node 2. As a result of the rotation, the Oγ of S16 (cyan sphere) forms a contact with the Nδ2 of N33 (green) in conformer 2. In contrast, the Oγ of S16 (blue sphere) forms a contact with the Nε2 of Q6 (brown) in conformer 1. The flipping of the side chain of Q6 (brown and ocher) is detected at node 5. Besides K15, the rigid body of node 8 also contains the side chain of I14 (red and orange spheres in Fig. 4e). The small movement of I14 correlates with the SCR motion of M12 (purple and pink) at node 9. In conformer 1, the Cε atom of M12 (purple sphere) is surrounded by hydrophobic atoms: Cγ2 (T8), Cδ2 (L9), Cδ1 (I46) (black spheres) and Cδ1 (I14), which are all within 4.0 Å. In conformer 2, the hydrophobic atoms are dispersed and their distances from the Cε atom of M12 are 5–10 Å. This example demonstrates that a series of SCR motions are coupled with the domain motion and this coupling is detected by AAMT.

Cluster of coupled SCR motions

The coupling of a number of SCR motions at the domain motion reminds us of a hypothetical mechanism of allosteric regulation: the binding of an effector molecule influences a spatially distant (allosteric) site through many side chain motions [22–24]. We collected 91 clusters of coupled SCR motions from the dataset, regardless of their coupling with the domain motion, and calculated the maximum distance between atoms within the cluster. The maximal distances were plotted against the cluster size (Fig. 5) because larger clusters contain distantly located atom pairs. Reference distances are introduced to evaluate whether the coupling of SCR motions is directional or not. We selected 10,000 sequential fragments randomly from the PDB and calculated the distances of the most separated atom pairs in the fragments. The average distance of the 10,000 fragments is shown as a line and the dispersion as a grey area in Figure 5. Maximal distances in the clusters (crosses) are mostly within the grey area. This shows that the clusters of SCR motions

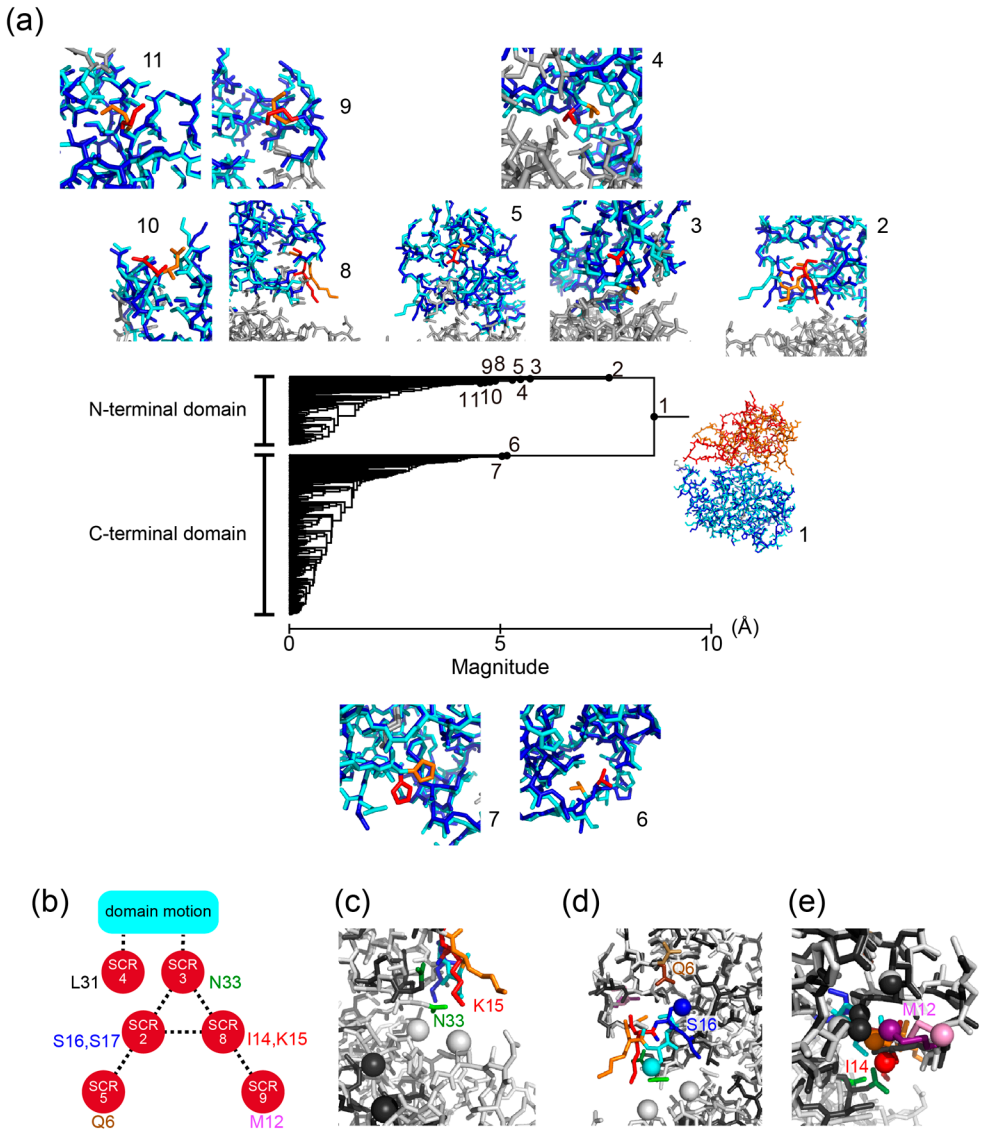

Figure 4 Structural change of the disulfide bond isomerase DsbC. (a) AAMT of DsbC. The motions at the effective nodes are shown in the same manner as Figure 1. (b) Schematic diagram of coupled SCR motions (motions at nodes 2, 3, 4, 5, 8 and 9). (c)–(e) The illustrations of coupled motions in the cluster. The motion at node 2 is highlighted in blue (conformation 1) and cyan colors (2). Motion 3 is shown in dark green (1) and green (2), motion 5 is shown in brown (1) and ocher (2), motion 8 is shown in red (1) and orange (2), and motion 9 is shown in purple (1) and pink (2). The other part is shown in black (1) and gray (2). Important atoms are presented as spheres.

require almost the same number of residues in the random fragments to transmit motions by couplings; the coupled SCR motions are not sufficiently efficient to reach allosteric sites when compared with those of random fragments. Note that, however, the current result is based on a dataset that exhibits simple domain motion. The application of AAMT to allosteric proteins and the analysis of coupled motions represent a potential future work.

We are confident that AAMT is a promising tool to investigate further coupling of global and local motions in proteins and for evaluating their consistency with function [25], in addition to analyze trajectories of molecular dynamics simulations [26,27] and large structural complexes [28].

Acknowledgments

This work was supported by a Grant-in Aid for Scientific Research on Innovative Areas “Molecular Engine” (JSPS KAKENHI Grant Number JP19H05390) to RK and by a Grant-in Aid for Scientific Research (B) (JP18H03331) to MO.

Conflicts of interest

The authors declare that they have no conflict of interest.

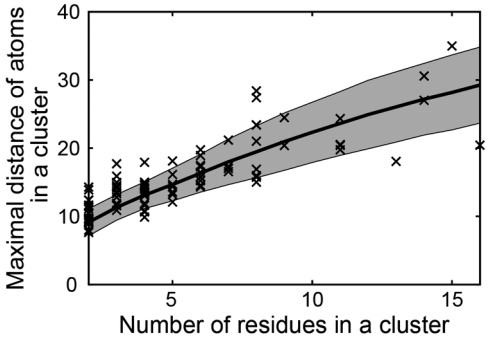

Figure 5 The maximal atom distance in a cluster of SCR motions (crosses). The average distances from the reference set and the standard deviations are shown by a black line and grey area, respectively. For example, in the disulfide bond isomerase DsbC (Fig. 4), the cluster composed of seven residues (Fig. 4b) gives the maximal distance 16.6 Å.

Author contributions

R. K. and M. O. directed the entire project and co-wrote the manuscript.

References

[1] Abrahams, J. P., Leslie, A. G., Lutter, R. & Walker, J. E. Structure at 2.8 Â resolution of F_1-ATPase from bovine heart mitochondria. *Nature* **370**, 621–628 (1994).
[2] Baldwin, J. & Chothia, C. Haemoglobin: the structural changes related to ligand binding and its allosteric mechanism. *J. Mol. Biol.* **129**, 175–220 (1979).
[3] Oda, T., Iwasa, M., Aihara, T., Maeda, Y. & Narita, A. The nature of the globular- to fibrous-actin transition. *Nature* **457**, 441–445 (2009).
[4] Toyoshima, C. & Nomura, H. Structural changes in the calcium pump accompanying the dissociation of calcium. *Nature* **418**, 605–611 (2002).
[5] Kinjo, A. R., Bekker, G. J., Suzuki, H., Tsuchiya, Y., Kawabata, T., Ikegawa, Y., *et al.* Protein Data Bank Japan (PDBj): updated user interfaces, resource description framework, analysis tools for large structures. *Nucleic Acids Res.* **45**, D282–D288 (2017).
[6] Kinjo, A. R., Bekker, G. J., Wako, H., Endo, S., Tsuchiya, Y., Sato, H., *et al.* New tools and functions in data-out activities at Protein Data Bank Japan (PDBj). *Protein Sci.* **27**, 95–102 (2018).
[7] Abyzov, A., Bjornson, R., Felipe, M. & Gerstein, M. RigidFinder: a fast and sensitive method to detect rigid blocks in large macromolecular complexes. *Proteins* **78**, 309–324 (2010).
[8] Boutonnet, N. S., Rooman, M. J. & Wodak, S. J. Automatic analysis of protein conformational changes by multiple linkage clustering. *J. Mol. Biol.* **253**, 633–647 (1995).
[9] Hayward, S. & Berendsen, H. J. Systematic analysis of domain motions in proteins from conformational change: new results on citrate synthase and T4 lysozyme. *Proteins* **30**, 144–154 (1998).
[10] Hayward, S., Kitao, A. & Berendsen, H. J. Model-free methods of analyzing domain motions in proteins from simulation: a comparison of normal mode analysis and molecular dynamics simulation of lysozyme. *Proteins* **27**, 425–437 (1997).
[11] Koike, R., Ota, M. & Kidera, A. Hierarchical description and extensive classification of protein structural changes by Motion Tree. *J. Mol. Biol.* **426**, 752–762 (2014).
[12] Nichols, W. L., Rose, G. D., Ten Eyck, L. F. & Zimm, B. H. Rigid domains in proteins: an algorithmic approach to their identification. *Proteins* **23**, 38–48 (1995).
[13] Ponzoni, L., Polles, G., Carnevale, V. & Micheletti, C. SPECTRUS: A Dimensionality Reduction Approach for Identifying Dynamical Domains in Protein Complexes from Limited Structural Datasets. *Structure* **23**, 1516–1525 (2015).
[14] Poornam, G. P., Matsumoto, A., Ishida, H. & Hayward, S. A method for the analysis of domain movements in large biomolecular complexes. *Proteins* **76**, 201–212 (2009).
[15] Sim, J., Sim, J., Park, E. & Lee, J. Method for identification of rigid domains and hinge residues in proteins based on exhaustive enumeration. *Proteins* **83**, 1054–1067 (2015).
[16] Wriggers, W. & Schulten, K. Protein domain movements: detection of rigid domains and visualization of hinges in comparisons of atomic coordinates. *Proteins* **29**, 1–14 (1997).
[17] Nishikawa, K., Ooi, T., Isogai, Y. & Saitô, N. Tertiary Structure of Proteins. I. Representation and Computation of the Conformations. *J. Physical Soc. Japan* **32**, 1331–1337 (1972).
[18] Kotting, C., Kallenbach, A., Suveyzdis, Y., Wittinghofer, A. & Gerwert, K. The GAP arginine finger movement into the catalytic site of Ras increases the activation entropy. *Proc. Natl. Acad. Sci. USA* **105**, 6260–6265 (2008).
[19] Dennis, C. C., Glykos, N. M., Parsons, M. R. & Phillips, S. E. The structure of AhrC, the arginine repressor/activator protein from Bacillus subtilis. *Acta Crystallogr D, Biol. Crystallogr.* **58**, 421–430 (2002).
[20] Haebel, P. W., Goldstone, D., Katzen, F., Beckwith, J. & Metcalf, P. The disulfide bond isomerase DsbC is activated by an immunoglobulin-fold thiol oxidoreductase: crystal structure of the DsbC-DsbDalpha complex. *EMBO J.* **21**, 4774–4784 (2002).
[21] Banaszak, K., Mechin, I., Frost, G. & Rypniewski, W. Structure of the reduced disulfide-bond isomerase DsbC from Escherichia coli. *Acta Crystallogr D, Biol. Crystallogr.* **60**, 1747–1752 (2004).
[22] Cui, Q. & Karplus, M. Allostery and cooperativity revisited. *Protein Sci.* **17**, 1295–1307 (2008).
[23] Lee, J. & Goodey, N. M. Catalytic contributions from remote regions of enzyme structure. *Chem. Rev.* **111**, 7595–7624 (2011).
[24] Nussinov, R. & Tsai, C. J. Allostery in disease and in drug discovery. *Cell* **153**, 293–305 (2013).
[25] Gō, N. Theoretical studies of protein folding. *Annu. Rev. Biophys Bioeng.* **12**, 183–210 (1983).
[26] Koike, R., Takeda, S., Maeda, Y. & Ota, M. Comprehensive analysis of motions in molecular dynamics trajectories of the actin capping protein and its inhibitor complexes. *Proteins* **84**, 948–956 (2016).
[27] Moritsugu, K., Koike, R., Yamada, K., Kato, H. & Kidera, A. Motion Tree Delineates Hierarchical Structure of Protein Dynamics Observed in Molecular Dynamics Simulation. *PLoS One* **10**, e0131583 (2015).
[28] Koike, R., Amemiya, T., Horii, T. & Ota, M. Structural changes of homodimers in the PDB. *J. Struct. Biol.* **202**, 42–50 (2018).

This article is licensed under the Creative Commons Attribution-NonCommercial-ShareAlike 4.0 International License. To view a copy of this license, visit https://creativecommons.org/licenses/by-nc-sa/4.0/.